AIAA 82-4207

Transonic Flow in the Throat Region of Annular Supersonic Nozzles

J. C. Dutton*
Texas A&M University, College Station, Texas
and
A. L. Addy†
University of Illinois at Urbana-Champaign, Urbana, Ill.

A theoretical and experimental investigation of flow in the throat region of annular supersonic nozzles has been conducted. The theoretical analysis consists of the formulation and development of an approximate, series expansion solution to the inviscid, irrotational governing equations. The resulting solution provides a direct means of analyzing the throat flowfields in a variety of two-dimensional nozzle configurations including axisymmetric, planar, and annular nozzles. Flowfield static pressure measurements have been obtained for four nozzle configurations, including a conventional axisymmetric nozzle and three annular ones. Half-section cylindrical models were constructed and mounted on a splitter plate whose surface corresponds to a plane of symmetry for the axisymmetric geometries under consideration. Measurements from a grid of pressure taps arranged on the splitter plate allowed the determination of the static pressure fields in the nozzle throats. For all four cases tested, it is found that the agreement between the theoretical and experimental results is quite good through a significant region of the throat. Only near the bounding walls in the throat inlet region is there a noticeable discrepancy for some of the cases.

Nomenclature

a	= speed of sound
d	= throat wall separation distance, Fig. 1
g,h	= equations of wall contours in x-y coordinate system, Fig. 1
g_1,h_1,g_2,h_2	= quantities defined in Eq. (19)
G,H	= equations of wall contours in R-Z coordinate system, Fig. 1
M	= Mach number
$\mathcal{O}$	= order of magnitude symbol
P	= pressure
R,Z	= cylindrical coordinate system, Fig. 1
R_c	= dimensionless throat wall radius of curvature
Re_{2d}	= Reynolds number based on sonic conditions and $2d$ length
T	= temperature
u,v	= dimensionless velocity components in x-y coordinates, Fig. 1 and Eqs. (5) and (6)
$\tilde{u},\tilde{v}$	= transonic perturbation velocity components, Eqs. (8) and (9)
u_1,v_1,u_2,v_2 u_3,v_3	= transonic perturbation velocity components, Eqs. (20) and (21)
U,V	= velocity components in R-Z coordinate system, Fig. 1
x,y	= dimensionless local coordinates, Fig. 1 and Eqs. (3) and (4)
z	= stretched axial coordinate, Eq. (19)
Z^*	= Z coordinate of x-y origin, Fig. 1
β	= angle of inclination of x axis from Z axis of symmetry, Fig. 1
β_1	= dimensionless inclination angle, Eq. (19)
γ	= specific heat ratio
ϵ	= expansion parameter, Eq. (18)
η	= parameter in expansion variable, Eq. (18)

Subscripts and Superscripts

i,o	= refers to inner and outer wall, respectively
0	= stagnation
$\bar{()}$	= average
$()^*$	= evaluated at sonic conditions

Received Oct. 2, 1981; revision received Jan. 26, 1982.

*Assistant Professor, Department of Mechanical Engineering. Member AIAA.

†Professor and Associate Head, Department of Mechanical and Industrial Engineering. Associate Fellow AIAA.

Introduction

ANNULAR supersonic nozzles constitute an integral part of a number of devices of practical importance. These applications include turbofan bypass nozzles; unconventional propulsion nozzles such as the spike, plug, and expansion-deflection designs; supersonic ejector systems; axial-flow aerodynamic windows; as well as the use of coaxial supersonic streams to obtain jet noise suppression. In order to analyze the inviscid, supersonic flowfield in the diverging portion of these nozzles, using a steady method of characteristics or finite difference technique, an accurate supersonic initial value line is required. One natural place to start these calculations is in the throat region of the nozzles, using an appropriate analysis of the transonic flowfield which occurs there. Given a slightly supersonic start line from the transonic analysis, the marching-type computations for the remainder of the nozzle flowfield can then proceed in the streamwise direction.

Several methods have been utilized to analyze transonic flow in the throat region of annular supersonic nozzles, including inverse techniques,[1,2] series expansion methods,[3-6] the method of integral relations,[7] time-dependent numerical techniques,[8-11] and numerical relaxation.[12] The inverse techniques require iteration for the direct problem of analyzing the flowfield in a nozzle with given inner and outer wall contours. In addition, previous series expansion and integral relations methods are restricted to specialized annular configurations, e.g., those with cylindrical centerbodies, or having large throat wall radii of curvature, or those whose

throats are located a large distance from the axis of symmetry. Because of their generality, the numerical techniques provide an attractive means of analyzing nozzle throat flowfields. In the time-dependent methods, the mixed nature of the governing equations for steady, inviscid, transonic flow is avoided by utilizing the unsteady form of the equations. In the type-dependent relaxation method utilized by Brown et al.,[12] the axial derivatives are approximated by centered differences in the subsonic portion of the flowfield and by backward differences in the supersonic region. Early efforts with the time-dependent technique were hampered by extremely long computing times. However, the recent time-dependent methods of Cline[10] and Chang[11] and the type-dependent relaxation technique of Brown et al.[12] have demonstrated the possibility of calculating annular nozzle throat flowfields with reasonable amounts of computer time.

The analytical technique presented here is a direct, series expansion method. A drawback of the expansion technique is that it assumes that the flow in the throat region is dependent only on the local wall radius of curvature and specific heat ratio of the gas and is, therefore, independent of the nozzle inlet geometry and rotational flow effects generated at the nozzle walls. However, the extensive series of measurements of Back et al.[13] suggests that the latter two effects are of secondary importance in the throat region. The resulting solution may be applied to a variety of annular nozzle configurations, including those for which the centerbody and outer wall contours are both curved or, alternately, those for which one boundary is straight. In addition, the throat wall radii of curvature can be relatively small, and the main flow direction may be either parallel or inclined with respect to the axis of symmetry. In the limit as the centerbody radius approaches zero and the outer wall, respectively, the solutions for the simpler cases of axisymmetric and planar nozzles are obtained. As a series expansion solution, it provides a fast and straightforward alternative to the previously mentioned numerical techniques for accurately analyzing many annular nozzle geometries of interest. Because of the speed and reliability of its numerical implementation, parametric studies and iterative calculations are facilitated.

Due to the difficulties encountered in obtaining disturbance-free measurements in internal, transonic flowfields, data for axisymmetric configurations in general, and the annular configuration in particular, are extremely sparse. For the axisymmetric-no-centerbody case, only Cuffel et al.[14] are known to have obtained flowfield data, i.e., measurements other than static wall pressure readings. This was accomplished by means of a small diameter tube with a static pressure hole drilled radially in it which was traversed through the nozzle throat. For the annular case, Bresnahan and Johns[15] and Liddle[7] measured static pressures along one wall of the nozzle throat region. No other previous investigations are known to have obtained measurements in the flowfield of annular nozzles. Thus, a second objective of this paper is to present flowfield data which have been obtained for an axisymmetric nozzle and three annular configurations. These measurements serve not only to broaden the existing data base, but they also provide a basis of comparison for the expansion solution which has been developed.

For an in-depth survey of the general topic of nozzle throat flows, Ref. 16 provides a useful review of early work, while the more recent surveys of Refs. 17-19 consider newer developments in this area.

Theory

Formulation and Series Solution

The series expansion technique is similar to that used by Hall[20] and Thompson and Flack.[5,6] Referring to Fig. 1, the configuration to be analyzed consists of an annular supersonic nozzle which, in general, may be inclined with respect to the axis of symmetry. The R-Z coordinate system is the standard cylindrical system, while the x-y coordinate system is rotated such that the y axis lies along the cross section of minimum area in the nozzle throat. The angle β is the inclination angle between the x and Z axes, and d is the distance in the R-Z coordinate system between the inner and outer throat wall locations. The coordinates of these last two points as well as those of the x-y origin and the equations of the inner and outer wall contours are also given in both the R-Z and x-y coordinate systems in the figure. It is to be noted that for the general case of an inclined, annular nozzle the minimum area cross section does not correspond to the cross section of minimum distance between the nozzle walls but rather lies nearer the axis of symmetry.

Under the assumptions of steady, inviscid, irrotational, adiabatic flow of a perfect gas, the governing equations are taken as the irrotationality condition and the gas dynamic equation

$$U_R - V_Z = 0 \tag{1}$$

$$(U^2 - a^2)\,U_Z + (V^2 - a^2)\,V_R + 2UVU_R - a^2 V/R = 0 \tag{2}$$

where a is the speed of sound and the subscripts are used to denote partial differentiation. Transforming from the R-Z to the rotated x-y coordinate system, where lengths are nondimensionalized with respect to the throat separation distance, d, and velocities with respect to the critical speed of sound, a^*,

$$x = \frac{(Z - Z^*)}{d}\cos\beta + \frac{R}{d}\sin\beta \tag{3}$$

$$y = -\frac{(Z - Z^*)}{d}\sin\beta + \frac{R}{d}\cos\beta \tag{4}$$

$$u = \frac{U}{a^*}\cos\beta + \frac{V}{a^*}\sin\beta \tag{5}$$

$$v = -\frac{U}{a^*}\sin\beta + \frac{V}{a^*}\cos\beta \tag{6}$$

using the adiabatic energy relation

$$\left(\frac{a}{a^*}\right)^2 = \frac{\gamma+1}{2} - \frac{\gamma-1}{2}(u^2 + v^2) \tag{7}$$

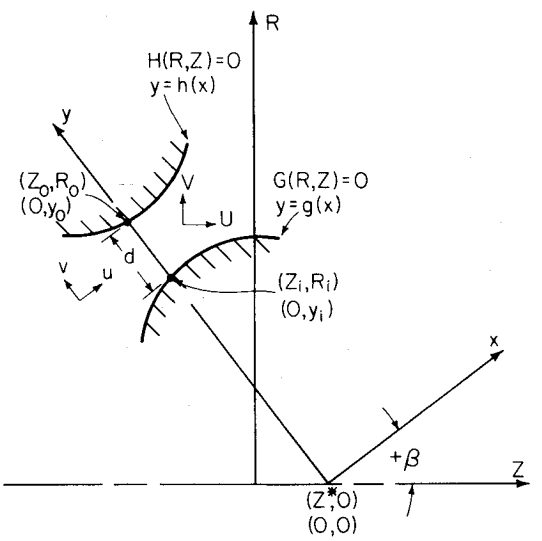

Fig. 1 Configuration for throat flowfield analysis of annular supersonic nozzles.

and introducing the transonic perturbation velocity components $\tilde{u}$ and $\tilde{v}$ by

$$u = 1 + \tilde{u} \tag{8}$$

$$v = \tilde{v} \tag{9}$$

Eqs. (1) and (2) take the form

$$\tilde{u}_y - \tilde{v}_x = 0 \tag{10}$$

$$\left(-2\tilde{u} - \tilde{u}^2 - \frac{\gamma-1}{\gamma+1}\tilde{v}^2\right)\tilde{u}_x - \frac{4}{\gamma+1}(1+\tilde{u})\tilde{v}\tilde{u}_y + \left(\frac{2}{\gamma+1} - \tilde{v}^2 - 2\frac{\gamma-1}{\gamma+1}\tilde{u} - \frac{\gamma-1}{\gamma+1}\tilde{u}^2\right)\tilde{v}_y + \left\{\left(\frac{2}{\gamma+1} - 2\frac{\gamma-1}{\gamma+1}\tilde{u} - \frac{\gamma-1}{\gamma+1}\tilde{u}^2 - \frac{\gamma-1}{\gamma+1}\tilde{v}^2\right)[\tilde{v} + (1+\tilde{u})\tan\beta]\right\}\Big/(y + x\tan\beta) = 0 \tag{11}$$

The boundary conditions in this inviscid analysis are that the nozzle walls must be streamlines. With $y = g(x)$ and $y = h(x)$ as the functional forms of the equations for the inner and outer wall contours in the meridional plane, the boundary conditions can be stated as

$$\tilde{v}[x, g(x)] = \{1 + \tilde{u}[x, g(x)]\}g'(x) \tag{12}$$

$$\tilde{v}[x, h(x)] = \{1 + \tilde{u}[x, h(x)]\}h'(x) \tag{13}$$

where the prime represents differentiation with respect to x. Expanding the equations for the contours in Maclaurin series about the throat and evaluating $g'(x)$ and $h'(x)$, the boundary conditions become

$$\tilde{v}[x, g(x)] = \{1 + \tilde{u}[x, g(x)]\}[g'(0) + g''(0)x + g'''(0)(x^2/2!) + \ldots] \tag{14}$$

$$\tilde{v}[x, h(x)] = \{1 + \tilde{u}[x, h(x)]\}[h'(0) + h''(0)x + h'''(0)(x^2/2!) + \ldots] \tag{15}$$

At this point in the analysis an expansion parameter, ϵ, must be chosen so that the perturbation velocity components can be expanded in appropriate series and substituted into the governing equations and boundary conditions. The expansion parameter used in this investigation is

$$\epsilon = (\bar{R}_c + \eta)^{-1} \tag{16}$$

where $\bar{R}_c$ is an average dimensionless radius of curvature for the two bounding walls. The value of the parameter η is arbitrary, and it is included[5,6,21] in order to improve the convergence properties of the series solution for nozzles with small wall radii of curvature. For $\eta > 1$, ϵ is less than unity regardless of how small $\bar{R}_c$ may be. Defining $\bar{R}_c$ in terms of the second derivatives of the wall contour equations,

$$\bar{R}_c \equiv \frac{2}{h''(0) - g''(0)} \tag{17}$$

the definition of ϵ employed in the solution is

$$\epsilon = \frac{h''(0) - g''(0)}{2 + \eta[h''(0) - g''(0)]} \tag{18}$$

Note that for a symmetric nozzle, $g''(0) = -h''(0)$ so that $\bar{R}_c$ reduces to $\bar{R}_c = 1/h''(0)$, as expected.

Investigating the order of magnitude of the quantities of interest using the dominant terms in Eqs. (10), (11), (14), and (15), a one-dimensional expression for the acceleration at the throat, and the definition of ϵ, it is found that $\tilde{u} = \mathcal{O}(\epsilon)$, $\tilde{v} = \mathcal{O}(\epsilon^{3/2})$, and, for consistency, that $x = \mathcal{O}(\epsilon^{1/2})$ and $\tan\beta/y = \mathcal{O}(\epsilon^{3/2})$. The estimate for x requires that attention be restricted to the transonic region near the throat plane, $x = 0$. Because of the estimate for $\tan\beta/y$, only small angles of inclination may be considered for annular nozzles with throats that are near the axis of symmetry in a dimensionless sense, $y = \mathcal{O}(1)$. However, this does not seem to be a serious restriction since one would not expect to encounter annular configurations for which the throat is very close to the symmetry axis, while the main flow x direction is highly inclined to it. For nozzles whose throats are large distances from the axis of symmetry, $y \gg 1$, the restriction to small angles of inclination may be relaxed as long as the previously mentioned estimate is satisfied. Obviously, however, radial flow configurations for which $\tan\beta \to \infty$ cannot be analyzed with this method.

In a similar manner the orders of magnitude of the Maclaurin series coefficients of the wall contour equations can be examined. Using circular arcs as models for the contour equations, it is found that $g'(0)$, $h'(0) = \mathcal{O}(\epsilon^{3/2})$; $g''(0)$, $h''(0) = \mathcal{O}(\epsilon)$; $g'''(0)$, $h'''(0) = \mathcal{O}(\epsilon^{7/2})$, etc. While these results apply specifically to nozzles with circular arc contours, the series solution is also valid for nozzles with other contours if their Maclaurin series coefficients have similar orders of magnitude.

Using these estimates, the following $\mathcal{O}(1)$ quantities are defined:

$$z \equiv \left[\frac{\gamma+1}{2}\epsilon\right]^{-1/2} x \qquad \beta_1 \equiv \left[\frac{\gamma+1}{2}\right]^{-1/2} \epsilon^{-3/2}\tan\beta$$

$$g_1 \equiv \left[\frac{\gamma+1}{2}\right]^{-1/2} \epsilon^{-3/2} g'(0) \qquad h_1 \equiv \left[\frac{\gamma+1}{2}\right]^{-1/2} \epsilon^{-3/2} h'(0)$$

$$g_2 \equiv \frac{2g''(0)}{h''(0) - g''(0)} \qquad h_2 \equiv \frac{2h''(0)}{h''(0) - g''(0)} \tag{19}$$

and the perturbation velocity components are expanded as

$$\tilde{u}(z,y) = u_1(z,y)\epsilon + u_2(z,y)\epsilon^2 + u_3(z,y)\epsilon^3 + \ldots \tag{20}$$

$$\tilde{v}(z,y) = \left[\frac{\gamma+1}{2}\epsilon\right]^{1/2} [v_1(z,y)\epsilon + v_2(z,y)\epsilon^2 + v_3(z,y)\epsilon^3 + \ldots] \tag{21}$$

Note in particular the transformation from axial coordinate x to the $\mathcal{O}(1)$, stretched coordinate z.

Substituting definitions (19) and expansions (20) and (21) into governing equations (10) and (11) and gathering coefficients of like powers of ϵ results in the following series of irrotationality and gas dynamic equations:

$$\frac{\partial u_n}{\partial y} - \frac{\partial v_n}{\partial z} = 0 \qquad n = 1,2,3,\ldots \tag{22}$$

and

$$-2u_1\frac{\partial u_1}{\partial z} + \frac{\partial v_1}{\partial y} + \frac{\beta_1 + v_1}{y} = 0 \qquad n = 1 \tag{23}$$

$$-2u_1\frac{\partial u_n}{\partial z} - 2u_n\frac{\partial u_1}{\partial z} + \frac{\partial v_n}{\partial y} + \frac{v_n}{y} = f_n(u_1, v_1, \ldots, u_{n-1}, v_{n-1}) \qquad n = 2,3,\ldots \tag{24}$$

where the functions, f_n, on the right-hand side of Eq. (24) are always known from lower order solutions and are listed in Ref. 19. Similar substitutions into Eq. (14) result in the series

of inner wall boundary conditions

$$v_1(z,y_i) = g_1 + g_2 z \tag{25}$$

$$v_2(z,y_i) = g_2 \eta z + (g_1 + g_2 z) u_1(z,y_i) \tag{26}$$

$$v_3(z,y_i) = g_2 \eta^2 z + g_2 \eta z u_1(z,y_i) + (g_1 + g_2 z) u_2(z,y_i) - \left(\frac{\gamma+1}{2}\right)(g_1 z + \tfrac{1}{2} g_2 z^2) \frac{\partial v_1}{\partial y}\bigg|_{y=y_i} \tag{27}$$

while substitution into Eq. (15) gives the outer wall boundary conditions as

$$v_1(z,y_o) = h_1 + h_2 z \tag{28}$$

$$v_2(z,y_o) = h_2 \eta z + (h_1 + h_2 z) u_1(z,y_o) \tag{29}$$

$$v_3(z,y_o) = h_2 \eta^2 z + h_2 \eta z u_1(z,y_o) + (h_1 + h_2 z) u_2(z,y_o) - \left(\frac{\gamma+1}{2}\right)(h_1 z + \tfrac{1}{2} h_2 z^2) \frac{\partial v_1}{\partial y}\bigg|_{y=y_o} \tag{30}$$

In obtaining the boundary conditions, the quantities $\bar{u}$ and $\bar{v}$ evaluated along the contours $y=g(x)$ and $y=h(x)$ are first expanded in Taylor series about the throat locations y_i and y_o. For curved contours, therefore, these conditions are satisfied exactly only at y_i and y_o, although for straight contours the boundary conditions are satisfied identically along the entire contour.

Equations (22-24) subject to conditions (25-30) are the ones which must be solved in order to obtain the perturbation velocity components. The method of solution utilizes assumed forms suggested by the boundary conditions and has been carried to the third order. The result is an algebraically complicated set of constants and functions, too long to be included herein, which yields the perturbation velocity components. Once these quantities have been determined, all other dependent variables of interest can be found, including the velocity components, Mach number, local static-to-stagnation pressure ratio, nozzle discharge coefficient, etc. Because of the closed-form nature of the series solution, these quantities can be rapidly evaluated in a straightforward manner. The TRANNOZ computer program[22] has been developed for this purpose. A solution summary and further details concerning the analysis are contained in Ref. 19.

Solution Checks and Parametric Studies

Due to the algebraic complexity of the series solution, a thorough series of tests has been performed to ensure its validity. The first set of tests involves reducing the solution for the general annular configuration to previous solutions for simpler geometries. The results for the conventional axisymmetric configuration are found by passing to the limit $y_i \to 0$ for a nozzle with a cylindrical centerbody, i.e., as the centerbody radius approaches zero. In this case the result of Hall[20] (with corrections by Kliegel and Levine[21]) for $\eta = 0$ and those of Ref. 23 for arbitrary η are recovered. Likewise the planar symmetric geometry may be investigated by allowing the centerbody to approach the outer nozzle wall, i.e., $y_i \to \infty$,§ since in this limit the axisymmetric effect becomes negligible. The general annular solution is found to correctly reduce to the plane results of Hall[20] for $\eta = 0$ and to the $\epsilon = (R_c + 1)^{-1}$ solution of Thompson and Flack[5,6] for $\eta = 1$.

The second group of tests involves numerically back-substituting the solutions for the various orders into the corresponding governing equations, Eqs. (22-24), and boundary conditions, Eqs. (25-30), and evaluating the residuals at various points in the nozzle throat. The partial derivatives in these equations are approximated by using second order, central, finite differences for all z derivatives and for y derivatives at interior points, and either forward or backward second order differences for the y derivatives at boundary points. In all cases the series solution is found to satisfy Eqs. (22-30), thus verifying the mechanics of obtaining the solution given its formulation.

In addition to the solution checks, a series of studies has been performed to investigate the effects of the parameter η, the nozzle geometry, and the solution order on the convergence properties of the series. As expected from the definition of the expansion variable, Eq. (18), the geometrical parameters which are by far the most influential are the radii

§In numerically reducing the annular solution to the planar limit, y_i cannot be made arbitrarily large since roundoff error occurs in the arithmetic evaluations. Using double precision on a CDC Cyber 175 computer, the upper limit for y_i is roughly 1000, which provides a very close approximation to the plane configuration.

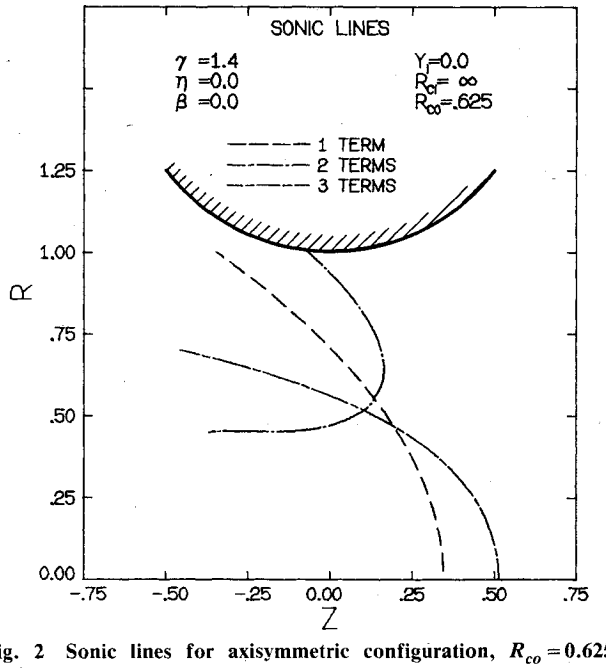

Fig. 2 Sonic lines for axisymmetric configuration, $R_{co} = 0.625$, $\eta = 0$.

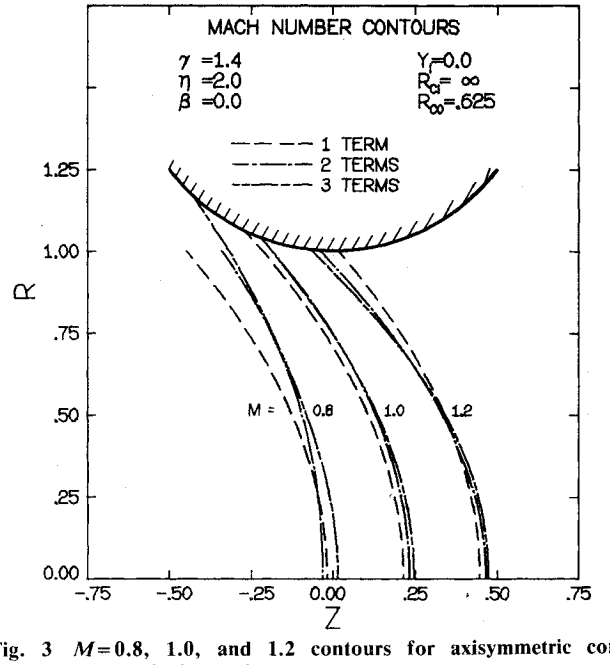

Fig. 3 $M = 0.8$, 1.0, and 1.2 contours for axisymmetric configuration, $R_{co} = 0.625$, $\eta = 2$.

of curvature of the bounding walls. For nozzles with large throat wall radii of curvature, it is found that the third order constant Mach number contours are essentially identical for various values of η. For nozzles with small $\bar{R}_c$, the convergence of the solutions is improved as η is increased. For example, Fig. 2 shows that for a conventional axisymmetric nozzle with a dimensionless outer wall radius of curvature $R_{co}=0.625$, the $\eta=0$ sonic lines are highly divergent. For $\eta=2$, on the other hand, the solution is much more well-behaved, as shown in Fig. 3. This improvement in convergence is obtained somewhat at the expense of satisfying the exact boundary conditions, Eqs. (12) and (13), although this effect can be ameliorated by utilizing third order solutions. Based on these studies it is recommended that third order, $\eta=2$, solutions be employed.¶ With this choice of solution order and η it is found that nozzle geometries with an average wall radius of curvature as small as $\bar{R}_c=0.5$ can be successfully analyzed as long as attention is restricted to a narrow region about the throat plane. For larger values of $\bar{R}_c$, the region through which the series solution can be accurately applied widens.

It has been remarked that the method utilized in this work is similar in nature to the one used by Thompson and Flack.[5,6] However, there are several important differences which make the solution presented here a more useful and powerful result. First, although the same expansion variable has been employed, the parameter η has not been limited to the values of zero and unity in this work as in Refs. 5 and 6. As has just been discussed, one of the conclusions of the parametric studies is that the best overall solution behavior is obtained when $\eta=2$ is utilized. In addition, the present solution exactly matches the first derivatives of the wall contour equations [$g'(0)$ and $h'(0)$] for all values of η. Also, no approximate methods for handling extra half-power terms in the expansions are necessary since no such terms are encountered. However, the primary advantage of the present solution is that in expanding the axisymmetric term in the gas dynamic equation [last term on the left-hand side of Eq. (11)], no assumptions have been made concerning the magnitude of the dimensionless distance from the axis of symmetry to the annular nozzle throat. Although this greatly complicates the analysis, once the solution has been obtained, it can be applied to the entire range of annular geometries from the conventional axisymmetric one to the planar one as the centerbody radius ranges from zero to a value which approaches the outer nozzle wall. In contrast, the solution of Thompson and Flack[5,6] assumes that the nozzle throat is located a large distance from the axis of symmetry so that only those cases may be analyzed.

Experiments

Equipment and Procedure

Rather than using the stretched tube technique employed in Ref. 14, the method utilized in this study was to construct and mount half-section models on a splitter plate whose surface corresponds to a symmetry plane. By placing static pressure taps on the splitter plate in the nozzle throat region, the flowfield pressure distributions could be obtained.

Obviously, the splitter plate technique does not perfectly model the corresponding full axisymmetric geometry because of the boundary layers which grow both on the plate and in the corners where the half-models meet the plate. However, for the high Reynolds number, favorable pressure gradient, nozzle flows under consideration, the boundary layers in the throat region are extremely thin. Although no boundary layer measurements were obtained during the course of the experimentation, sample calculations using the code developed in Ref. 24 show that, for the models and typical operating conditions used here, the boundary layer displacement thickness is expected to be less than 0.2% of the throat diameter in all cases. It is therefore felt that the measurements obtained with the half-section models correspond closely to the "true" measurements for the full axisymmetric configurations.

Figure 4 shows a half-section drawing of one of the annular configurations which has been tested. Note in particular the R-Z cylindrical coordinate system; this is the system used in the presentation of the data. The Z axis of symmetry lies on the splitter plate surface and the origin is chosen such that the R axis passes through the center of curvature of the outer nozzle wall. These coordinates are made dimensionless with respect to the radial distance to the minimum point on the outer wall contour (25.4 mm). In the configuration shown, the center of curvature of the centerbody lies along the $Z=0$ plane. The other two annular configurations are obtained by translating the centerbody such that its center of curvature lies along the planes $Z=+0.5$ and $Z=-0.5$. The conventional axisymmetric geometry is obtained by removing the cen-

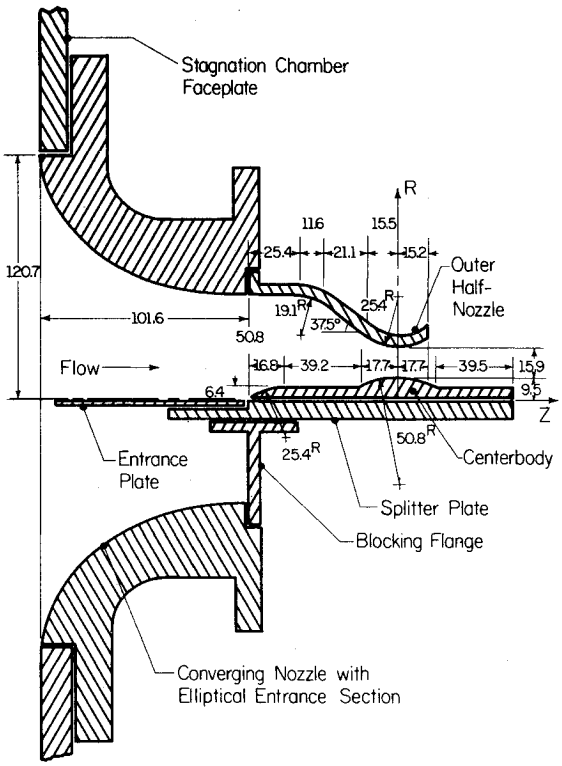

Fig. 4 Half-section drawing of annular axisymmetric experimental configuration; all dimensions are in millimeters.

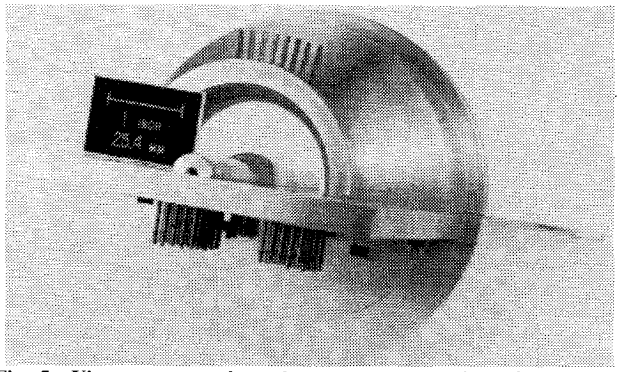

Fig. 5 View upstream through measurement region of assembled, half-section, annular nozzle.

¶This value of η is equivalent to the value $\eta=1$ recommended in Ref. 23 for the axisymmetric nozzle. Because of the difference in the expansion parameters employed in the two solutions, values of η in the present work are twice as large as the equivalent values from Ref. 23.

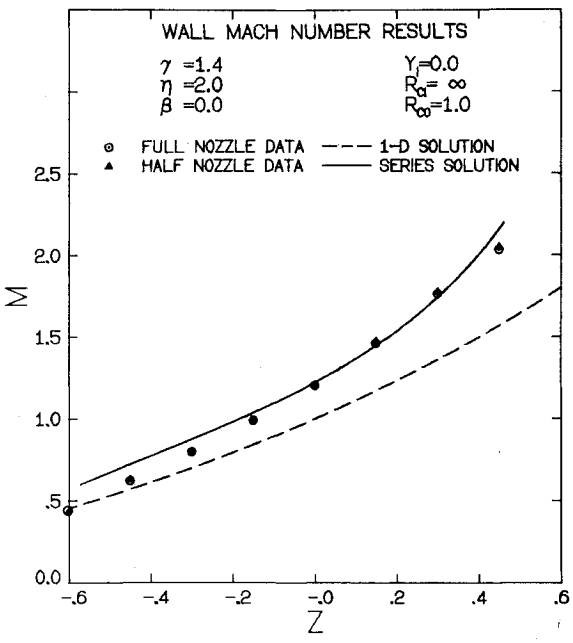

Fig. 6 Comparison of full- and half-section wall Mach number measurements with one-dimensional solution and series expansion solution for a conventional axisymmetric nozzle; $Re_{2d} = 2.68 \times 10^6$, $P_0 = 350.3$ kPa, $T_0 = 289$ K for full nozzle and $Re_{2d} = 3.09 \times 10^6$, $P_0 = 402.8$ kPa, $T_0 = 289$ K for half nozzle experiments.

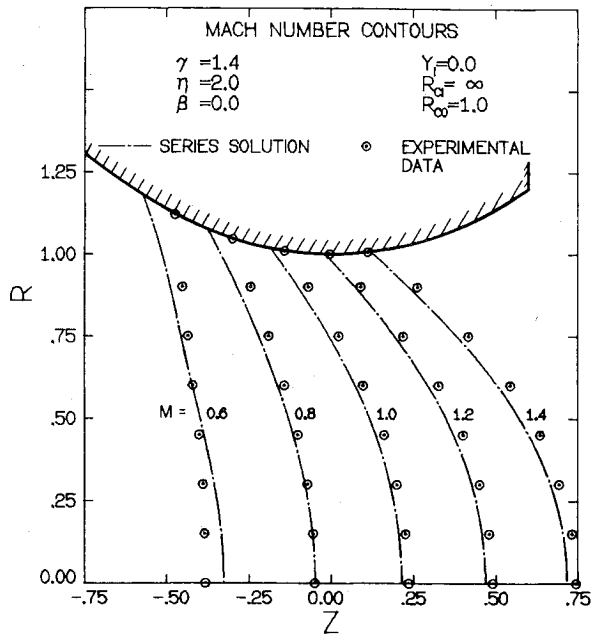

Fig. 7 Comparison of constant Mach number contours from series expansion solution with experimental data for conventional axisymmetric nozzle; $Re_{2d} = 3.04 \times 10^6$, $P_0 = 397.9$ kPa, $T_0 = 289$ K for experiments.

terbody. Dry, filtered, compressed air is supplied to the test section from a large stagnation chamber at the left in Fig. 4. The flow is then accelerated through a converging nozzle with an elliptical contour before reaching the annular supersonic nozzle section. From there the flow exhausts to the facility silencing system.

The stagnation chamber pressure and the test section static pressures were measured with a strain gage transducer/digital output system in conjunction with a 48-port, motor-driven Scanivalve. A photograph of the half-section annular nozzle assembly, which views the measurement region from the downstream side, is shown in Fig. 5. The grid of pressure taps used to obtain the flowfield static pressure and outer wall pressure distributions is clearly visible. The shorter row of taps seen below the splitter plate passes through a slot in the plate and is attached to the centerbody for measurement of its wall pressure distribution. For the annular nozzle configurations, a total of 67 pressure taps were available for the measurements while for the axisymmetric nozzle, 79 total taps were used. Once these pressure measurements were obtained they were converted to contours of constant Mach number by use of the isentropic relation and Hermite spline interpolation. The accuracy of the pressure measurements was within approximately ± 1.5 kPa which corresponds to a fractional uncertainty in the Mach number of $\pm 1.3\%$ at $M = 0.6$ and $\pm 0.6\%$ at $M = 1.4$. Mass flow measurements were not attempted in this series of experiments.

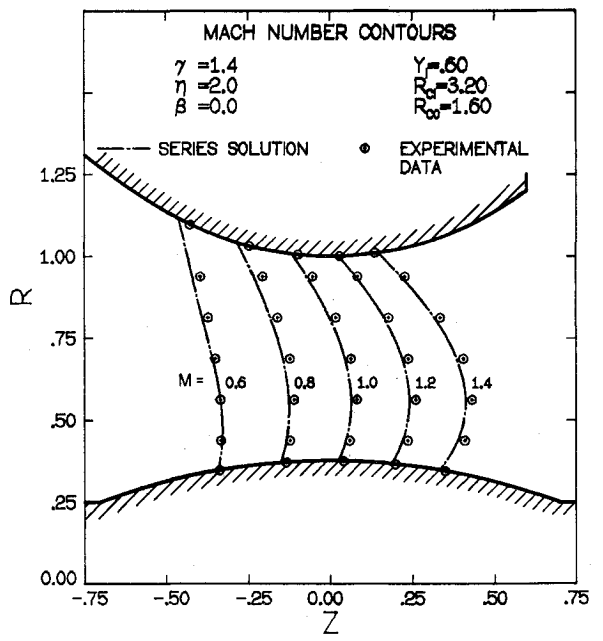

Fig. 8 Comparison of constant Mach number contours from series expansion solution with experimental data for annular nozzle with centerbody center of curvature along $Z = 0$ plane; $Re_{2d} = 1.96 \times 10^6$, $P_0 = 409.5$ kPa, $T_0 = 289$ K for experiments.

Comparisons to Theory

To test the hypothesis that the splitter plate boundary layer did not seriously affect the flowfield pressure measurements, a full-section conventional axisymmetric nozzle, $R_{ci} \to \infty$, was also designed and built. Comparison of the wall pressure measurements between this model and the corresponding half-model then allows conclusions to be drawn regarding the effects of this boundary layer. The two sets of measurements are compared in Fig. 6 where the pressure data has been converted to Mach numbers. Since the nozzle throat radius and wall radius of curvature are equal for this axisymmetric geometry, the value of R_{co} is 1.0. As can be seen, the experimental results for the two models are essentially identical, thus lending credence to the above-stated hypothesis. Also shown are the predictions of the annular nozzle series solution as well as that of one-dimensional theory. As recommended in the preceding section, third order, $\eta = 2$ series results are used. Near the throat plane, $Z = 0$, and on downstream, the series predictions are in fairly good agreement with the data. Upstream of the throat, however, there is disagreement which can be attributed to two major causes. First, at the furthest upstream taps the Mach number is relatively low, $M \cong 0.5$, so that the results of the transonic theory are not expected to agree with the data. Probably more important, though, is the fact that upstream of the $Z = -0.6$ station, the wall contour is

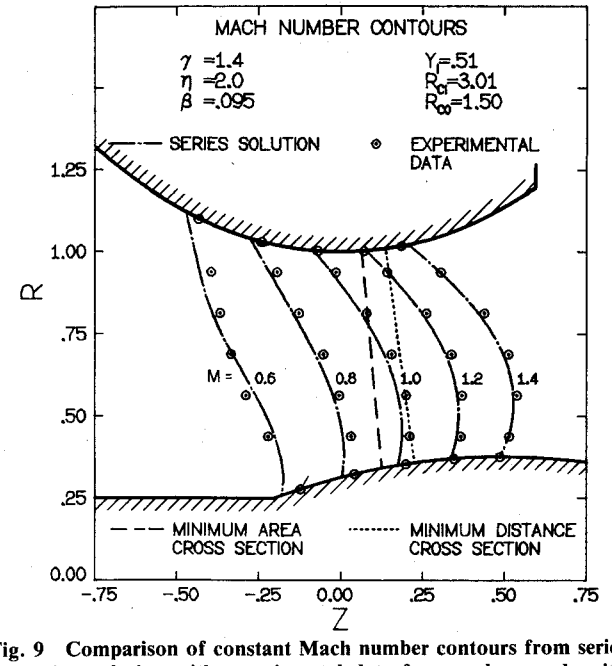

Fig. 9 Comparison of constant Mach number contours from series expansion solution with experimental data for annular nozzle with centerbody center of curvature along $Z=0.5$ plane; $Re_{2d}=2.08\times10^6$, $P_0=409.0$ kPa, $T_0=289$ K for experiments [flagged data point obtained by extrapolation].

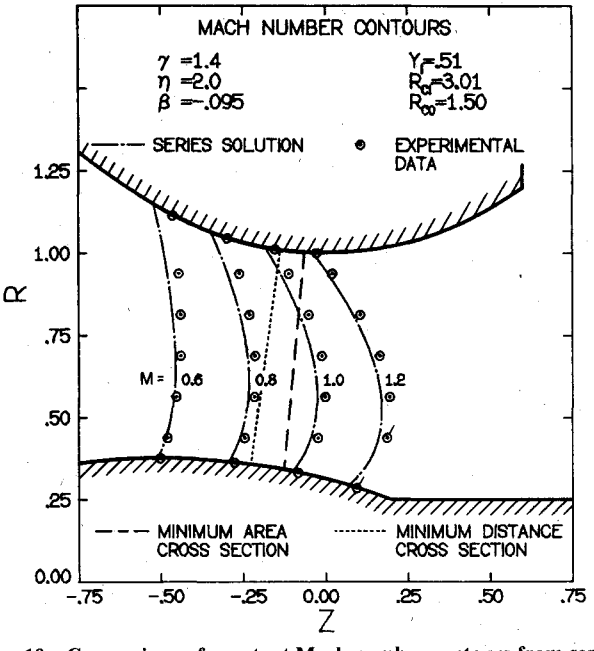

Fig. 10 Comparison of constant Mach number contours from series expansion solution with experimental data for annular nozzle with centerbody center of curvature along $Z=-0.5$ plane; $Re_{2d}=2.08\times10^6$, $P_0=408.2$ kPa, $T_0=289$ K for experiments [flagged data points obtained by extrapolation].

not a circular arc but rather is a 37.5 deg conically convergent section. Since this transition in the wall contour is not allowed for in the analysis, it is not surprising that the data and series results disagree near the tangency point. Except at the most upstream locations, the one-dimensional theory is seen to err seriously.

Figures 7-10 present the comparisons between the theoretical and experimental results for the throat iso-Mach contours in the four configurations investigated. Figure 7 contains the results for the conventional axisymmetric nozzle with $R_{co}=1.0$. In the annular case of Fig. 8 the centerbody center of curvature lies along the $Z=0$ plane so that the main flow direction is parallel to the axis of symmetry, $\beta=0$. The values for the dimensionless inner and outer wall throat radii of curvature and the y distance to the inner wall are $R_{ci}=3.2$, $R_{co}=1.6$, and $y_i=0.6$, respectively. In Fig. 9 the centerbody has been shifted downstream such that its center of curvature lies along the $Z=0.5$ plane. In this case the flow direction is inclined by $\beta=0.095$ rad away from the Z axis and $R_{ci}=3.01$, $R_{co}=1.50$, $y_i=0.51$. As previously mentioned, the minimum area throat cross section and the cross section of minimum distance between the walls (which connects their centers of curvature) do not coincide for inclined, annular nozzles. The two sections are marked in Fig. 9 and, as can be seen, there is a significant separation distance between the two. The configuration of Fig. 10 is obtained by moving the centerbody upstream so that its center of curvature lies along $Z=-0.5$. The values of the parameters are identical to those in Fig. 9 except that the flow is inclined toward the axis of symmetry, $\beta=-0.095$ rad.

It is seen that the agreement between the theoretical and experimental results is generally quite good except in the throat inlet regions, particularly near the walls. This can again be attributed to the fact that the series solution uses the circular arc contours of the central throat region in its evaluations and cannot account for the transitions which occur to the outer wall conical inlet and centerbody cylindrical inlet sections. It is also seen that the data generally lies slightly downstream from the theoretical predictions. Most likely this is due to the theory being an inviscid one while it is well known[25] that the effect of wall friction is to shift the sonic line downstream in a nozzle throat. In any event, the series expansion solution provides an accurate description of the flowfields through a surprisingly wide region of the nozzle throats.

Conclusions

A series expansion solution has been developed for transonic flow in the throat region of annular nozzles. The problem has been formulated in such a manner that the resulting solution may be correctly applied to the series of annular configurations ranging from the conventional axisymmetric geometry to the two-dimensional planar one as the centerbody radius is increased from zero and allowed to approach the outer nozzle wall. In addition, the flow direction may be inclined with respect to the axis of symmetry and the nozzle throat wall radii of curvature may be of the order of the throat wall separation distance, d, or larger. The results of this analysis have been compared to flowfield data obtained with the splitter plate technique for an axisymmetric and three annular nozzles. In general the agreement is very good except in the throat inlet regions where transitions in the wall contours of the experimental models occur. Because of the speed and reliability with which the series solution can be evaluated, it provides a convenient and accurate method of analyzing throat flowfields for a variety of annular configurations of interest. It may also be useful as an initial condition for the numerical time-dependent and relaxation techniques in order to speed their convergence.

Acknowledgment

Support for this research was provided in part by the U.S. Army Research Office under Research Grant DAAG 29-76-G-0200 and Research Contract DAAG 29-79-C-0184.

References

[1] Lord, W. T., "A Theoretical Study of Annular Supersonic Nozzles," Aeronautical Research Council, Reports and Memoranda No. 3227, Oct. 1959.

[2] Hopkins, D. F. and Hill, D. E., "Transonic Flow in Unconventional Nozzles," *AIAA Journal*, Vol. 6, May 1968, pp. 838-842.

[3]Moore, A. W. and Hall, I. M., "Transonic Flow in the Throat Region of an Annular Nozzle with an Arbitrary Smooth Profile," Aeronautical Research Council, Reports and Memoranda No. 3480, Jan. 1965.

[4]Smithey, W.J.H. and Naber, M. E., "Sonic Line for a Coaxial Axisymmetric Nozzle," *AIAA Journal*, Vol. 11, April 1973, pp. 569-570.

[5]Thompson, H. D. and Flack, R. D., "Transonic Flow Computation in Annular and Unsymmetric Two-Dimensional Nozzles," U.S. Army Missile Command Technical Rept. No. RD-73-21, Dec. 1973.

[6]Flack, R. D. and Thompson, H. D., "Comparison of Pressure and LDV Velocity Measurements with Predictions in Transonic Flow," *AIAA Journal*, Vol. 13, Jan. 1975, pp. 53-59.

[7]Liddle, S. G., "Integral Relations Method Computations of Annular and Asymmetric Plane Nozzle Flowfields," *Journal of Spacecraft and Rockets*, Vol. 11, March 1974, pp. 146-151.

[8]Laval, P., "Time-Dependent Calculation Method for Transonic Nozzle Flows," *Lecture Notes in Physics*, Vol. 8, Springer Verlag, New York, 1971, pp. 187-192.

[9]Serra, R. A., "Determination of Internal Gas Flows by a Transient Numerical Technique," *AIAA Journal*, Vol. 10, May 1972, pp. 603-611.

[10]Cline, M. C., "VNAP: A Computer Program for Computation of Two-Dimensional, Time-Dependent, Compressible, Viscous, Internal Flow," Los Alamos Scientific Laboratory Rept. LA-7326, Nov. 1978.

[11]Chang, I-S., "One- and Two-Phase Nozzle Flows," *AIAA Journal*, Vol. 18, Dec. 1980, pp. 1455-1461.

[12]Brown, E. F., Brecht, T.J.F., and Walsh, K. E., "A Relaxation Solution of Transonic Nozzle Flows Including Rotational Flow Effects," *Journal of Aircraft*, Vol. 14, Oct. 1977, pp. 944-951.

[13]Back, L. H., Massier, P. F., and Gier, H. L., "Comparison of Measured and Predicted Flows through Conical Supersonic Nozzles, with Emphasis on the Transonic Region," *AIAA Journal*, Vol. 3, Sept. 1965, pp. 1606-1614.

[14]Cuffel, R. F., Back, L. H., and Massier, P. F., "Transonic Flowfield in a Supersonic Nozzle with Small Throat Radius of Curvature," *AIAA Journal*, Vol. 7, July 1969, pp. 1364-1366.

[15]Bresnahan, D. L. and Johns, A. L., "Cold Flow Investigations of a Low Angle Turbojet Plug Nozzle with Fixed Throat and Translating Shroud at Mach Numbers from 0 to 2.0," NASA TM X-1619, Aug. 1968.

[16]Hall, I. M. and Sutton, E. P., "Transonic Flow in Ducts and Nozzles; a Survey," *Symposium Transsonicum*, Springer Verlag, Berlin, 1964, pp. 325-344.

[17]Flack, R. D. and Thompson, H. D., "An Experimental and Analytical Investigation of Internal Transonic Flow," U.S. Army Missile Command Technical Rept. No. RD-73-20, Oct. 1973.

[18]Brown, E. F. and Hamilton, G. L., "Survey of Methods for Exhaust-Nozzle Flow Analysis," *Journal of Aircraft*, Vol. 13, Jan. 1976, pp. 4-11.

[19]Dutton, J. C. and Addy, A. L., "A Theoretical and Experimental Investigation of Transonic Flow in the Throat Region of Annular Axisymmetric, Supersonic Nozzles," Dept. of Mechanical and Industrial Engineering, Univ. of Illinois at Urbana-Champaign, Rept. No. UILU-ENG-80-4001, Jan. 1980.

[20]Hall, I. M., "Transonic Flow in Two-Dimensional and Axially-Symmetric Nozzles," *Quarterly Journal of Mechanics and Applied Mathematics*, Vol. XV, Pt. 4, 1962, pp. 487-508.

[21]Kliegel, J. R. and Levine, J. N., "Transonic Flow in Small Throat Radius of Curvature Nozzles," *AIAA Journal*, Vol. 7, July 1969, pp. 1375-1378.

[22]Dutton, J. C. and Addy, A. L., "TRANNOZ: A Computer Program for Analysis of Transonic Throat Flow in Axisymmetric, Planar, and Annular Supersonic Nozzles," Dept. of Mechanical and Industrial Engineering, Univ. of Illinois at Urbana-Champaign, Rept. No. UILU-ENG-80-4005, April 1980.

[23]Dutton, J. C. and Addy, A. L., "Transonic Flow in the Throat Region of Axisymmetric Nozzles," *AIAA Journal*, Vol. 19, June 1981, pp. 801-804.

[24]Dutton, J. C. and Addy, A. L., "Theory, Computer Program, and Illustrative Examples for the Two-Dimensional Boundary Layer Flow of Ideal Gases," U.S. Army Missile R&D Command Tech. Rept. T-CR-78-10, March 1978.

[25]John, J.E.A., *Gas Dynamics*, 1st ed., Allyn and Bacon, Boston, 1969, pp. 174-176.